Localization of electrons and electromagnetic waves in a deterministic aperiodic system

Mihnea Dulea

Institute for Physics and Technology of Materials, P.O. Box MG-7, R-76900 Bucharest-Magurele, Romania

Magnus Johansson and Rolf Riklund

Department of Physics and Measurement Technology, University of Linköping, S-581 83 Linköping, Sweden

(Received 2 April 1991)

Electron localization and optical transmission in one-dimensional systems with two components distributed according to the Rudin-Shapiro sequence are investigated. The nature of the eigenstates in the diagonal tight-binding model is studied by making use of nonlinear recurrence relations satisfied by the associated transfer matrices and their traces. It is shown that the wave functions display a wide range of features going from weak to exponential localization. Numerical computations lead to the conjecture that the localization property is generic. Nevertheless, a countable dense set of critical values of the on-site potential amplitude is found for which a class of extended states exists. Accordingly, the numerical investigation of the time evolution of the electronic wave packets displays a subdiffusive behavior when the potential amplitude becomes critical. Finally, a study of the optical properties of the Rudin-Shapiro dielectric multilayer shows strong similarities with the behavior of the disordered multilayers regarding the development of gaps in the transmission spectra.

I. INTRODUCTION

The interest in the physical properties of deterministic aperiodic systems has increased explosively during the last years, especially since the experimental discovery of the quasicrystals.[1] Various models were conceived in order to explain the influence that the type of aperiodic atomic distribution has on their properties (for a review see, e.g., Ref. 2). Among the treated subjects, the localization problem plays a central role. Since it was rigorously proven in one dimension and is generally accepted in two and three dimensions that disorder can lead to electron localization, it is of great interest to know if different kinds of deterministic aperiodic systems can show the same property. The first step towards the answer was done in the frame of the study of incommensurate systems when electron localization was discovered in the Aubry model.[3] Another system displaying localization was later obtained by mapping the kicked quantum rotator into a one-dimensional tight-binding model with an unbounded incommensurate potential.[4] It is interesting to note that, in both models, the wave functions are exponentially localized but the localization length is energy independent in the first case, while it depends on the energy as in the Lloyd disordered model in the second case.

A class of models which has recently received much attention is the one characterized by distributions of components generated by substitutions or finite automata.[5] The results obtained in this field until now showed the existence of extended and recurrent (critical) electronic states[6,7,22] and a rich self-similar structure of the electromagnetic wave transmission spectra,[8-10] sometimes displaying a tendency towards the development of transmission bands.[9,10] In the frame of these studies, a question naturally arose: How close can the behavior of

an automatic system be to that of a disordered one? This paper intends to be a step towards the answer in regards to the localization of electrons and light by giving an example of an automatic distribution whose complexity generates physical properties which are qualitatively close to those existing in disordered structures. This is the case of the string containing two different components (letters) distributed in a deterministic and aperiodic way according to the Rudin-Shapiro (RS) sequence.[11] Even if it shares with the other automatic sequences the general feature of having zero configurational entropy, the RS sequence displays the additional remarkable property of possessing an absolutely continuous Fourier measure whose uniform density equals one, exactly like a random distribution.[12] This makes the RS system a natural candidate for the investigation of the possible similarities with the disordered systems.

Despite its interesting properties, the RS distribution was treated only scarcely in the physical literature, probably due to the inherent technical difficulties risen by the complexity of the problem. A few conjectures and results were published concerning the hopping conduction,[13] the distribution of gaps in the diagonal tight-binding model,[14] and the multifractal analysis of the Fourier transform.[15] The authors of Ref. 16 have recently derived a trace map for one-dimensional RS systems and conjectured some consequences this can have on the electronic spectrum of the associated tight-binding model.

Here the localization of electrons and electromagnetic waves in binary systems with the components distributed according to the RS sequence is investigated. The formalism of the transfer matrix is described and recurrence relations relating the transfer matrices and their traces corresponding to successive generations of the chain are derived in Sec. II. Section III is devoted to the study of the spectrum and wave functions of the diagonal tight-

binding model with site energies distributed according to the RS sequence. The dynamics of wave packets is investigated in Sec. IV. The last part of the article (Sec. V) treats the transmission of electromagnetic waves through a dielectric multilayer whose components are again ordered like the letters in the RS sequence.

II. DYNAMICAL MAPS

There are many equivalent ways to generate the RS sequence (see, e.g., Ref. 11). Here we adopt the substitutional procedure which is subsequently described. Fix a four letter alphabet $\{A,B,C,D\}$ and define a (concurrent) binary substitution relation acting on it given by

$$A \rightarrow AB , \tag{2.1a}$$

$$B \rightarrow AC , \tag{2.1b}$$

$$C \rightarrow DB , \tag{2.1c}$$

$$D \rightarrow DC . \tag{2.1d}$$

Take A as a seed and apply the substitution once. The two-letter word AB is obtained which will be called the first generation of the sequence. A straightforward recurrence procedure to obtain the pth generation by applying the substitution to each letter of the $(p-1)$th one can be defined in this way. The first few successive generations read

$$A \rightarrow AB \rightarrow AB\,AC \rightarrow AB\,AC\,ABDB \rightarrow AB\,AC\,ABDB\,AB\,ACDC\,AC \rightarrow \cdots . \tag{2.2}$$

The RS sequence is obtained when identifying each A or B with A, and each C or D with B in the above string, such that we finally get the generations

$$A \rightarrow A\,A \rightarrow A\,A\,AB \rightarrow A\,A\,AB\,A\,AB\,A \rightarrow A\,A\,AB\,A\,AB\,A\,A\,A\,ABBB\,AB \rightarrow \cdots . \tag{2.3}$$

The physical system studied in this section consists of a chain of atoms of two kinds distributed like the A's and B's in the RS sequence of letters. Each site A (B) has the energy V $(-V)$, and an electron with energy E can hop from site to site according to the following diagonal tight-binding equation of motion:

$$\psi_{n+1} + \psi_{n-1} + V_n \psi_n = E \psi_n , \tag{2.4}$$

where ψ_n denotes the wave amplitude on site n, $V_n = \pm V$, and the hopping integral is set equal to one. In what follows we will always consider a positive V.

The above system of equations can be written as

$$\underline{U}_{n+1} = \underline{M}_n \underline{U}_n, \quad \underline{U}_n \equiv \begin{bmatrix} \psi_n \\ \psi_{n-1} \end{bmatrix}, \quad \underline{M}_n \equiv \begin{bmatrix} E - V_n & -1 \\ 1 & 0 \end{bmatrix}, \tag{2.5}$$

where $\underline{M}_n$ is the unimodular transfer matrix associated with the site n. Then the total transfer matrix corresponding to the nth generation of the RS chain is given by

$$\underline{A}_n = \underline{M}_N \underline{M}_{N-1} \underline{M}_{N-2} \cdots \underline{M}_2 \underline{M}_1, \quad N = 2^n, \ n \ge 0 . $$

In analogy with these, we can define in the case of the four-letter sequence matrices $\underline{B}_n$, $\underline{C}_n$, and $\underline{D}_n$ through the following equations which are the direct consequence of the recurrence relation (2.1):

$$\underline{A}_{n+1} = \underline{B}_n \underline{A}_n , \tag{2.6a}$$

$$\underline{B}_{n+1} = \underline{C}_n \underline{A}_n , \tag{2.6b}$$

$$\underline{C}_{n+1} = \underline{B}_n \underline{D}_n , \tag{2.6c}$$

$$\underline{D}_{n+1} = \underline{C}_n \underline{D}_n , \tag{2.6d}$$

with

$$\underline{A}_0 = \underline{M}_A, \quad \underline{B}_0 = \underline{M}_A, \quad \underline{C}_0 = \underline{M}_B, \quad \underline{D}_0 = \underline{M}_B ,$$

where $\underline{M}_A$ $(\underline{M}_B)$ denotes the matrix $\underline{M}_n$ in (2.5) when V_n equals V $(-V)$. The above equations define a nonlinear 16-dimensional mapping for the entries of the matrices. If we take into account the unimodularity of the matrices, this dimension is reduced to 12. Moreover, the relations (2.6) are symmetric under the transformation which replaces all $\underline{A}_n$ with $\underline{D}_n$ and all $\underline{B}_n$ with $\underline{C}_n$. In the particular case of the tight-binding model, the equations lead to the following identities:

$$\underline{A}_n(E, V) = \underline{D}_n(E, -V), \quad \underline{B}_n(E, V) = \underline{C}_n(E, -V) . \tag{2.7}$$

The first equation above gives a physical meaning to $\underline{D}_n$; according to (2.7), $\underline{D}_n$ describes again the nth generation of the RS system but with V replaced by $-V$. For our purposes we would like to have an equation satisfied by matrices $\underline{A}_n$ (or $\underline{D}_n$) only. The necessary decoupling of the recurrence relations (2.6) is performed in the Appendix and its result reads

$$\underline{A}_{n+1} = \underline{A}_{n-1} \underline{A}_{n-2}^{-1} \underline{A}_{n-1} \underline{A}_{n-2}^{-2} \underline{A}_n \underline{A}_{n-1}^{-1} \underline{A}_{n-2}^{-1} \underline{A}_{n-1} \underline{A}_n , \tag{2.8}$$

$$\underline{C}_n = \underline{B}_{n-1} \underline{C}_{n-2} \underline{B}_{n-2}^{-1} \underline{C}_{n-1} . \tag{2.9}$$

Due to the above-mentioned symmetry, the matrices $\underline{D}_n$ satisfy a formula analogous to (2.8) and $\underline{B}_n$ an equation similar to (2.9) but with the $\underline{C}_n$'s replaced by $\underline{B}_n$'s and vice versa.

As proven in the Appendix, Eqs. (2.6) induce useful recurrence relations for the traces of the total transfer matrices, which read

$$a_{n+1} - d_{n+1} = a_n b_n - c_n d_n ,$$

$$b_{n+1} - c_{n+1} = a_n c_n - b_n d_n , \tag{2.10}$$

where the trace of the matrix $\underline{X}_n$ ($\underline{X} = \underline{A}, \underline{B}, \underline{C}, \underline{D}$) is denoted by x_n ($x = a, b, c, d$).

Relations similar to (2.10) appear in Ref. 16 where a complete eight-dimensional trace map was derived. The authors conjectured that the RS trace map has a structure similar to the Thue-Morse and copper-mean maps as regards the fractal structure of the basin of attraction and the nonexistence of a polynomial invariant. Here it will be shown that, despite these similarities, the physical properties of the RS systems in what concerns the spectral and optical behavior are qualitatively different. Equations (2.8)–(2.10) will be used in the next section for the study of some special wave functions.

III. SPECTRUM AND WAVE FUNCTIONS

This section is devoted to the study of the spectrum and nature of the wave functions of the RS diagonal tight-binding model described by Eq. (2.4). We investigate first the spectra of its periodic approximants obtained by repeating unit cells corresponding to the configurations of the successive generations. Then the parameter E belongs to the spectrum of the periodic approximant given by the nth generation if and only if it satisfies the condition

$$|\mathrm{tr}\underline{A}_n(E,V)| \le 2 . \qquad (3.1)$$

The trace of the total transfer matrix corresponding to the nth generation is a polynomial of order 2^n in the variables E and V. Then Eq. (3.1) says that the energies are the solutions of an algebraic inequality of degree 2^n. To derive a general expression for the above-mentioned polynomials is an impossible task even for simpler atomic distributions. Fortunately there are some particular cases which can be solved without too much difficulty. Suppose, for example, that for some values of E and V the traces corresponding to a given n satisfy the following equations:

$$a_n(E,V) = d_n(E,V), \quad b_n(E,V) = c_n(E,V) . \qquad (3.2)$$

Then it can easily be seen from the recurrence relations (2.10) that the same equalities hold for any index $m \ge n$. This means that the dynamics of the trace map is trapped when $m \ge n$ into the six-dimensional invariant subspace described in Ref. 16. The earliest generation for which Eqs. (3.2) are satisfied is the second one, in which case the value of the parameter E reads

$$E = \pm (V^2 + 2)^{1/2} . \qquad (3.3)$$

In the Appendix it is proven that, whenever E takes one of the above values, the total transfer matrices corresponding to the odd generations have the following expression:

$$\underline{A}_{2j+1} = \begin{bmatrix} f_j^2 - 1 - EF_j & F_j \\ -3F_j & f_j^2 - 1 + EF_j \end{bmatrix}, \quad j \ge 2 , \qquad (3.4)$$

where the polynomials f_j and F_j are defined by

$$f_{j+1} = 2^{1/2}(f_j^2 - 1), \quad j \ge 1 ,$$

$$f_1(V) = 2^{1/2}V , \qquad (3.5)$$

$$F_j = 2^{j/2} \prod_{r=1}^{j} f_r .$$

Moreover, the following identity is obtained as a direct consequence of the unimodularity of $\underline{A}_{2j+1}$:

$$f_j^2 = 2[1 + (V^2 - 1)F_{j-1}^2], \quad j \ge 1 . \qquad (3.6)$$

Equation (3.5) suggests the parametrization $V = (z + z^{-1})/2$, where z can be a positive real number (when $V \ge 1$) or a complex number with modulus one (when $V \le 1$). Then the following equalities hold:

$$f_j = 2^{-1/2}(z^{N_j - 1} + z^{-N_j - 1}), \quad N_j = 2^j, \quad j \ge 1 , \qquad (3.7)$$

$$F_j = S_{N_j - 1}(z), \quad j \ge 2 , \qquad (3.8)$$

$$a_{2j+1} = z^{N_j} + z^{-N_j}, \quad j \ge 2 , \qquad (3.9)$$

where $S_n(z)$ denotes the nth Chebyshev polynomial of the first kind.[17] If $V \le 1$, there is a θ in $[0, \pi/2]$ such that $V = \cos\theta$ and $a_{2j+1} = 2\cos(N_j\theta)$; that is, condition (3.1) is satisfied. On the other hand, $V > 1$ implies the divergence of the sequence of traces corresponding to the odd generations. In conclusion, when the condition (3.3) is satisfied, E belongs to the spectrum of the odd generations if and only if $V \le 1$, and gaps open when $V = 1$ at $E = \pm\sqrt{3}$. Moreover, whenever $V < 1$, Eqs. (3.4) and (3.7) say that the entries of the matrices $\underline{A}_{2j+1}$ are given by

$$(\underline{A}_{2j+1})_{11} = \cos(N_j\theta) - [(3 + V^2)/(1 - V^2)]^{1/2}\sin(N_j\theta) ,$$

$$(\underline{A}_{2j+1})_{12} = \sin(N_j\theta)/\sin\theta ,$$

$$(3.10)$$

$$(A_{2j+1})_{21} = -3(A_{2j+1})_{12} ,$$

$$(\underline{A}_{2j+1})_{22} = \cos(N_j\theta) + [(3 + V^2)/(1 - V^2)]^{1/2}\sin(N_j\theta) .$$

For a fixed V, the above formulas define bounded functions of argument j showing that, when applying the matrices $\underline{A}_{2j+1}$ to some arbitrary vector U_1 with unit norm,
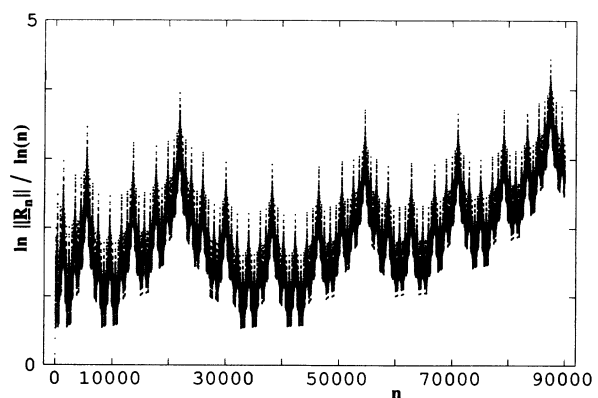

FIG. 1. The natural logarithm of $\|\underline{R}_n\|$ divided by the logarithm of the site index n for the case $V = 1$ and $E = -3^{1/2}$.
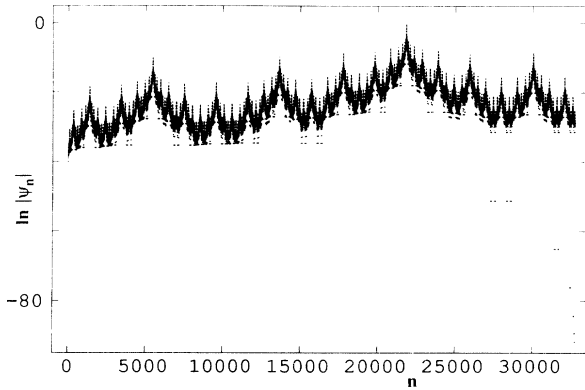
FIG. 2. The natural logarithm of the absolute value of the wave function coefficients ψ_n plotted as a function of the site index n for $V = 1$, $E = -1.732\,050\,807\ldots$ and $N = 32\,768$.

the sequence $\|U_{N_{2j+1}+1}\|$ of the norms of its iterates is bounded. A completely different picture is found for $V = 1$, in which case it can easily be seen from (3.4) and (A8) that the total transfer matrices read

$$\underline{A}_{2j+1} = \begin{bmatrix} 1 - EN_j & N_j \\ -E^2 N_j & 1 + EN_j \end{bmatrix} , \tag{3.11}$$

$$\underline{A}_{2j} = \begin{bmatrix} 1 - EN_j & EN_j^2 - 4N_j \\ N_j & 1 - N_j^2 + EN_j \end{bmatrix} . \tag{3.12}$$
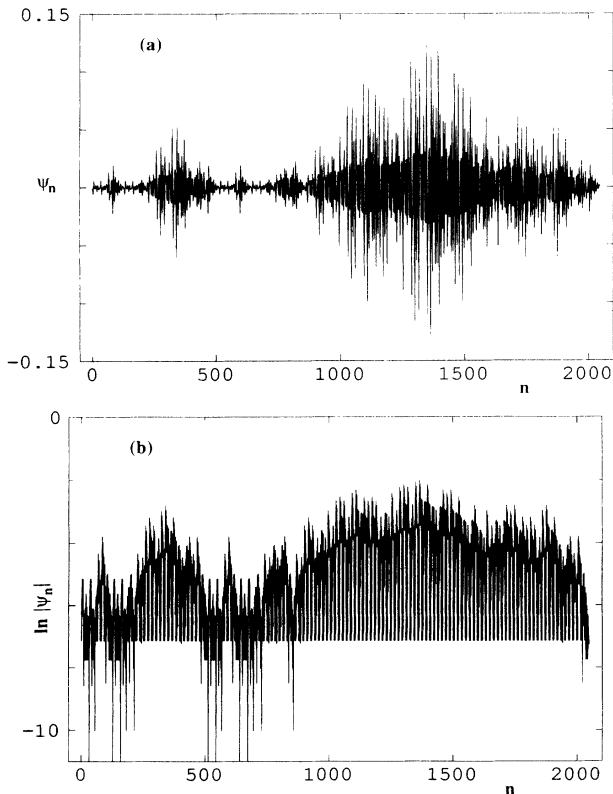
FIG. 3. (a) The wave-function coefficients ψ_n plotted as a function of site index n for $N = 2047$, $V = 2^{-1/2}$, and $E \approx -(V^2 + 2)^{1/2}$ using free boundary conditions. (b) Same as (a), but in logarithmic scale.

As a consequence of the above expressions, the wave functions corresponding to the energies given by (3.3) possess subsequences of power-law increasing amplitudes on sites N_j^2, $N_j^2 + 1$ (with power 1), and $2N_j^2$, $2N_j^2 + 1$ (with power $\frac{1}{2}$), $j \geq 1$. If we denote the products of transfer matrices by $\underline{R}_n \equiv \underline{M}_n \underline{M}_{n-1} \cdots \underline{M}_2 \underline{M}_1$, then a plot of $\ln(\|\underline{R}_n\|)/\ln(n)$ as a function of n (see Fig. 1) shows that the latter power-law behavior is, in fact, a lower bound. (Here, and whenever necessary, the computations were performed in multiple precision, the number of significant digits being chosen in each case such that numerical errors were practically eliminated.) An upper bound is given by the values of the amplitudes on sites labeled by the sequence of numbers $m_r = 8 + n_r$, $n_r = \sum_{j=2}^r N_{2j}$, $r \geq 2$. The first two relations from (2.6) can be used to prove the identity

$$\underline{R}_{n_r} = \underline{A}_4 \underline{A}_6 \cdots \underline{A}_{2r-2} \underline{A}_{2r} . \tag{3.13}$$

Then it follows from Eq. (3.12) that, for large r, the norms of the matrices $\underline{R}_{n_r}$ satisfy the scaling law

$$\|\underline{R}_{n_r}(E = \pm\sqrt{3}, V = 1)\| \sim \text{const} \times n_r^{\beta \ln(n_r) + \gamma} , \tag{3.14}$$

where numerical computations performed in multiple precision give $\beta = (4\ln 2)^{-1}$. In conclusion, the eigenfunctions corresponding to (3.3) are weaker than exponentially localized when $V = 1$. This pattern can clearly be seen when numerically computing the free boundary condition approximants (see Fig. 2). On the other hand, Eqs. (3.10) suggest a qualitative change in the nature of states when $V < 1$. An extreme situation appears when $V \equiv \cos\theta$ takes one of the critical values corresponding to those values of θ from $(0, \pi/2)$, which are integer multiples of π/N_j. If we assume that $\theta = k\pi/N_j$, $0 < k < N_j/2$, we obtain, with the help of (3.10) and (2.8),

$$\underline{A}_{2j+1} = (-1)^k \underline{I} ,$$

$$\underline{A}_{2j+2r+1} = \underline{I} , \tag{3.15}$$

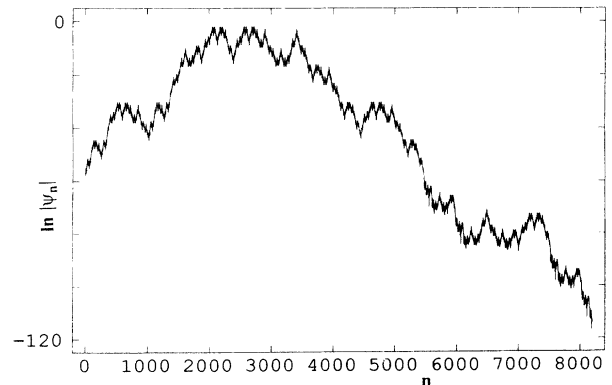$$\underline{A}_{2j+2r+2} = \underline{A}_{2j+2}^{2r}, \quad r \geq 1 ,$$

FIG. 4. The natural logarithm of the absolute value of the wave-function coefficients ψ_n plotted as a function of the site index n for $V = 1$, $E = -0.517\,638\,090\ldots$, $N = 8192$, using free boundary conditions.

where $\underline{I}$ denotes the identity matrix. In what follows we will study in detail the case $V=2^{-1/2}$ ($j=2$, $k=1$). Then, as proven in the Appendix, there is a periodic subsequence of sites (given by the set of indices $m_{p,q}=1+16p-4q$, $p=0,1,2,\ldots,q=0.1$) on which $|\psi_{m_{p,q}}|=|\psi_1|$. Moreover, numerical computations show that the sequence of norms of matrices $\underline{R}_n$ is again dominated by the subsequence $\|\underline{R}_{n_r}\|$ whose values can be computed with the help of (3.15). We obtain

FIG. 6. The state with lowest energy in a RS chain of length $N=2048$ with $V=1$ plotted in a logarithmic scale.

$$\underline{A}_{2r}=\begin{bmatrix} 1 & 0 \\ -2^{1/2}N_{r-1} & 1 \end{bmatrix},$$

(3.16)

$$\underline{R}_{n_r}=\underline{A}_4\begin{bmatrix} 1 & 0 \\ -(2^r-4)2^{1/2} & 1 \end{bmatrix},$$

which gives the scaling law

$$\|\underline{R}_{n_r}(E=\pm\sqrt{5}/\sqrt{2},V=1/\sqrt{2})\|\sim\text{const}\times n_r^{1/2} .$$

(3.17)

This allows us to conclude that, in the limit of the infinite

FIG. 5. (a) The normalized second moment, (b) the inverse participation ratio, and (c) the normalized first moment vs eigenenergy number for a Rudin-Shapiro chain with $V=1$ and the length $N=512$.
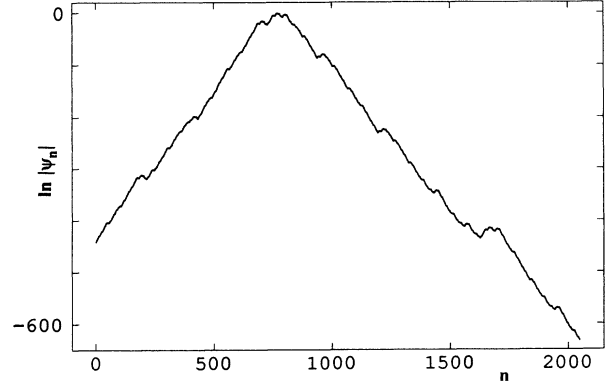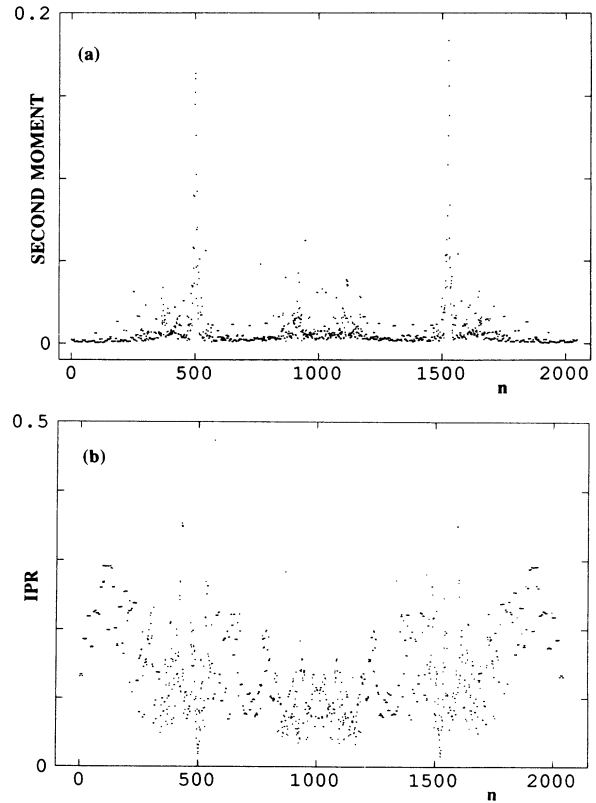

FIG. 7. (a) The normalized second moment and (b) inverse participation ratio vs eigenenergy number for a RS chain with $V=2^{-1/2}$ and the length $N=2047$.

chain, the wave function is non-normalizable, that is, extended. The derived features can be easily seen in Fig. 3.

The above argument can be extended to the other critical values of V, giving a whole class of extended functions possessing periodic subsequences of amplitudes whose periods depend on V. Also, it is to be noted that Eqs. (3.10) do not exclude the existence of extended states for other (noncritical) subunitary values of V whose energies satisfy (3.3), but their investigation is more complicated and will not be performed here.

A similar analysis can, in principle, be applied to other values of E and V which are simultaneous solutions of the relations (3.2) and (3.1) for odd $n \geq 3$ (e.g., $E = \pm[2 + (2 + V^4)^{1/2}]^{1/2}$ for $V = 1$ or $E = \pm[2 - (2 + V^4)^{1/2}]^{1/2}$ for $V = 1, 1/\sqrt{2}$). A plot of the associated wave functions calculated in multiple precision (see one example in Fig. 4) displays some very complex self-similar structures with an overall tendency towards localization.

A general picture of the nature of all the states [including those which do not satisfy the condition (3.2)] can be obtained by computing their first and second moments and the inverse participation ratio. The numerical computation performed for various values of V showed that the localization property is generic. This can be easily seen, for instance, in Figs. 5(a) and 5(b), where extremely small (large) values of the second moment (inverse participation ratio) are displayed. It is useful to remember that the second moment takes values greater than 0.18 for extended states and the inverse participation ratio gives the inverse of the number of sites that support the wave function. Moreover, a picture of the first moment of the states exhibit a completely disordered pattern, as in a random system [see Fig. 5(c)]. The analogy is even closer because a large class of typical exponentially localized states exist, exactly as in a purely random system (see Fig. 6).

The same analysis of the second moment and inverse participation ratio but for critical values of V reveals two bands of extended states around the energy values given by (3.3) (see Figs. 7).

IV. TIME EVOLUTION

The most appealing picture of localization is given by studying the time spreading of an initially localized wave packet. Unfortunately, its achievement demands the knowledge of both electronic spectrum and wave functions, raising serious analytical difficulties. This problem can be overcome by numerically diagonalizing large tight-binding Hamiltonians and by computing all the relevant quantities in the eigenvector representation. One quantity of interest is the mean-square displacement of the wave packet whose long-time behavior can give information concerning the extension of eigenstates. For a wave packet localized at $t = 0$ on the site n_0 of a chain this is given by

$$\langle [\Delta x(t)]^2 \rangle = \sum_n (n - n_0)^2 |\psi_n(t)|^2 . \qquad (4.1)$$

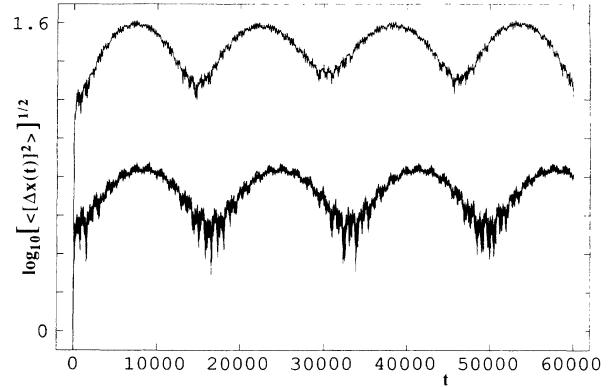In the long-time limit the square root of this quantity is

FIG. 8. The time evolution of the logarithm of the root-mean-square deviation $[\langle [\Delta x(t)]^2 \rangle]^{1/2}$ plotted for two different values of the site energy amplitude V, $V = 1.0$ (upper), and $V = 2.0$ (lower), for a Rudin-Shapiro chain. The length of the chain is $N = 2047$ and the electron was located at site $(N-1)/2 = 1023$ at time $t = 0$.

known to behave like t^α, where $\alpha = 1$ for extended states in periodic lattices, $\alpha = \frac{1}{2}$ for extended states in disordered systems and $\alpha = 0$ for localized states in random lattices. Recent studies on aperiodic chains[18] have displayed a rich variety in behavior: while in the Aubry model α equals one or zero if the potential amplitude is smaller, respectively, greater than a critical value, in the Fibonacci case α takes values in the range $(0,1)$ depending again on the site energy amplitude. Superdiffusive behavior $(\alpha > \frac{1}{2})$ has also been found in a random-dimer model,[19] and in Ref. 20 it has been proven that the diffusive spread of the wave packet can take place only if the spectrum is singular continuous. The numerical results obtained here for the RS lattice will show that, in concordance with the study performed in the previous chapter, the existence of very few extended states in a sea of localized ones can slightly increase the value of α from zero to small positive values, leading to subdiffusive dynamics.

The explicit form of the time-dependent wave function in the representation of the energy eigenstates $|k\rangle$ reads
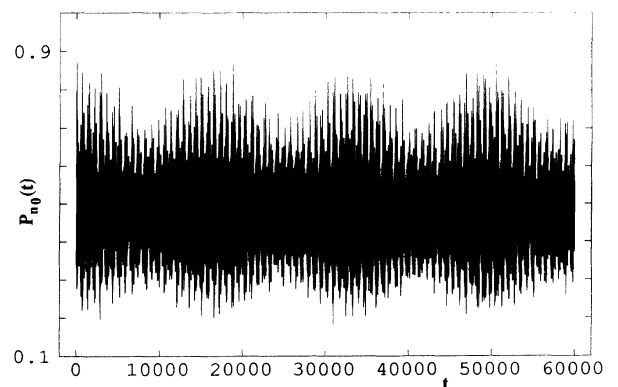

FIG. 9. The probability of return $P_{n_0}(t)$ for a Rudin-Shapiro chain of length 2047 and $V = 2$ with starting site $n_0 = 1023$.
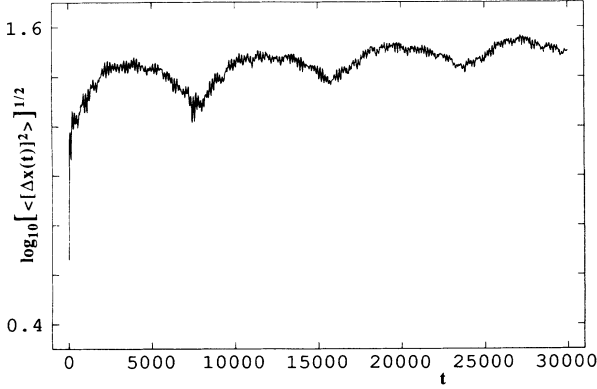
FIG. 10. The same as in Fig. 8 but with $V=2^{-1/2}(1+2^{-1/2})^{1/2}$.

$$|\psi(t)\rangle = \sum_m \sum_k \exp(-iE_k t)\langle k|m\rangle \psi_m(t=0)|k\rangle , \qquad (4.2)$$

where $\langle m|k\rangle$ denotes the amplitude of $|k\rangle$ on the site m. Equations (4.1) and (4.2) show that only those eigenstates having nonzero amplitudes in the region where the wave packet was localized at $t=0$ contribute to the mean-square displacement. If all these eigenstates are localized, then the wave packet will never reach the boundary of the system and will oscillate quasiperiodically at large times between two limit positions, giving in the mean the value zero for the exponent α.

Another quantity of interest is the probability of return of the particle into the region where it was initially localized. The strict positivity of this quantity in the asymptotic long-time regime was the first localization criterion used by Anderson in his classical study of the disordered solid.[21] If the particle was initially localized on the site n_0, the probability of return has the following simple expression:

$$P_{n_0}(t) = |\psi_{n_0}(t)|^2 \qquad (4.3)$$

and can be computed explicitly with the help of (4.2).

In what follows we will discuss the long-time asymptotical dynamics of one electron initially localized near the middle of the RS lattice. When all the eigenstates are localized, the dynamics of the wave packet width displays a
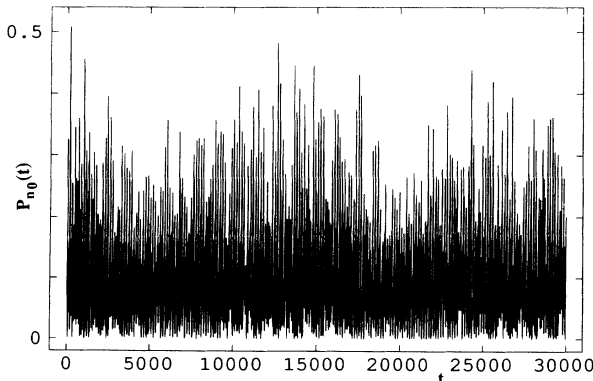

FIG. 11. The same as in Fig. 9 but with V as in Fig. 10.

superposition of oscillations with different time scales around a straight line with slope $\alpha=0$ (see Fig. 8). According to (4.1) and (4.2), the largest period which can be seen in Fig. 8 for a fixed V is proportional to the reciprocal of the smallest spacing between the energies associated to the class of states which supports the motion. The probability of return at the starting site shows symmetric oscillations around a relatively high value (see Fig. 9).

When V takes a critical value and the initial site is chosen such that the amplitude of at least one extended state at this site has a considerable magnitude, the above picture changes qualitatively. Such an example is given in Fig. 10, where the positive slope of the packet width is clearly seen (the corresponding value of α computed from the asymptotics with the least-squares method is here 0.12). Moreover, the probability of return displayed in Fig. 11 is slightly decreasing and its mean value is shifted towards smaller values, showing a slow spreading of the wave packet onto the lattice.

V. OPTICAL TRANSMISSION

The system which we analyze in this section consists of a dielectric multilayer constructed from two components A and B characterized by refractive indices n_A and n_B respectively. The components are again distributed following the RS string. The multilayer is inserted between two half-infinite media of type A and the layer thicknesses are adjusted such that the variation of the phase of the normally incident beam is the same in both kinds of layers. Then it can be shown[8,10] that the values of the electrical field and its first derivative at the interface of two successive layers are components of some vectors which satisfy an equation similar to (2.5), the matrices $\underline{M}_n$ being given this time by

$$\underline{M}_n = \begin{bmatrix} \cos\delta & -r_n^{-1}\sin\delta \\ r_n\sin\delta & \cos\delta \end{bmatrix} . \qquad (5.1)$$

In the above equation, δ denotes the phase variation through one layer and r_n equals 1 if the nth layer is of type A, or n_A/n_B if it is of type B.

The transmission coefficient T_n through a system containing 2^n layers distributed according to the nth generation of the chain is related to the entries m_{ij} of the total transfer matrix through the equation[8,10]

$$4[T_n(\delta)]^{-1} - 2 = m_{11}^2 + m_{12}^2 + m_{21}^2 + m_{22}^2 . \qquad (5.2)$$

The numerical computations performed for the same refractive indices but different number of layers show the development of transmission gaps around the phase values $\delta = \delta_k = (2k+1)\pi/2$ when increasing the generation number (here k denotes any integer number). As seen in Figs. 12(a) and 12(b) the behavior of $T_n(\delta_k)$ depends strongly on n: the even generations give transmission maxima while the values corresponding to the odd ones vanish exponentially when the number of layers increases to infinity. This can be explained easily if we compute the first three matrices $\underline{A}_n(\delta_k)$ ($n=1,2,3$) and then apply mathematical induction in order to obtain

with the help of the recurrence relation (2.8) the following general expression:

$$\underline{A}_{2n+1}(\delta_k)=\underline{I}, \quad \underline{A}_{2n}=\begin{bmatrix} r^{-N} & 0 \\ 0 & r^N \end{bmatrix}, \quad n\geq 3, \qquad (5.3)$$

where $r=n_A/n_B$ and $N=2^{n-1}$. Therefore, the transmission coefficient will, in this case, take the values one or $4/[2+(r^{2N}+r^{-2N})]$ only.

If we compare the above-mentioned transmission spectra for the RS chain with the spectra corresponding to the same refractive indices but various disordered layer distributions obtained with a random number generator, we can observe the development of similar gaps around

the values $\delta=\delta_k$ [see Figs. 12(c)–12(f)]. This feature common to the disordered and RS layers seems to be the opposite of the behavior of the Thue-Morse and of the copper-mean class of quasiperiodic systems (obtained by generalizing the Fibonaccian sequence) previously reported,[9,10] which develop transmission bands around the same values of the phase.

VI. SUMMARY

The localization of the electrons and electromagnetic waves in binary structures with components distributed according to the deterministic aperiodic Rudin-Shapiro
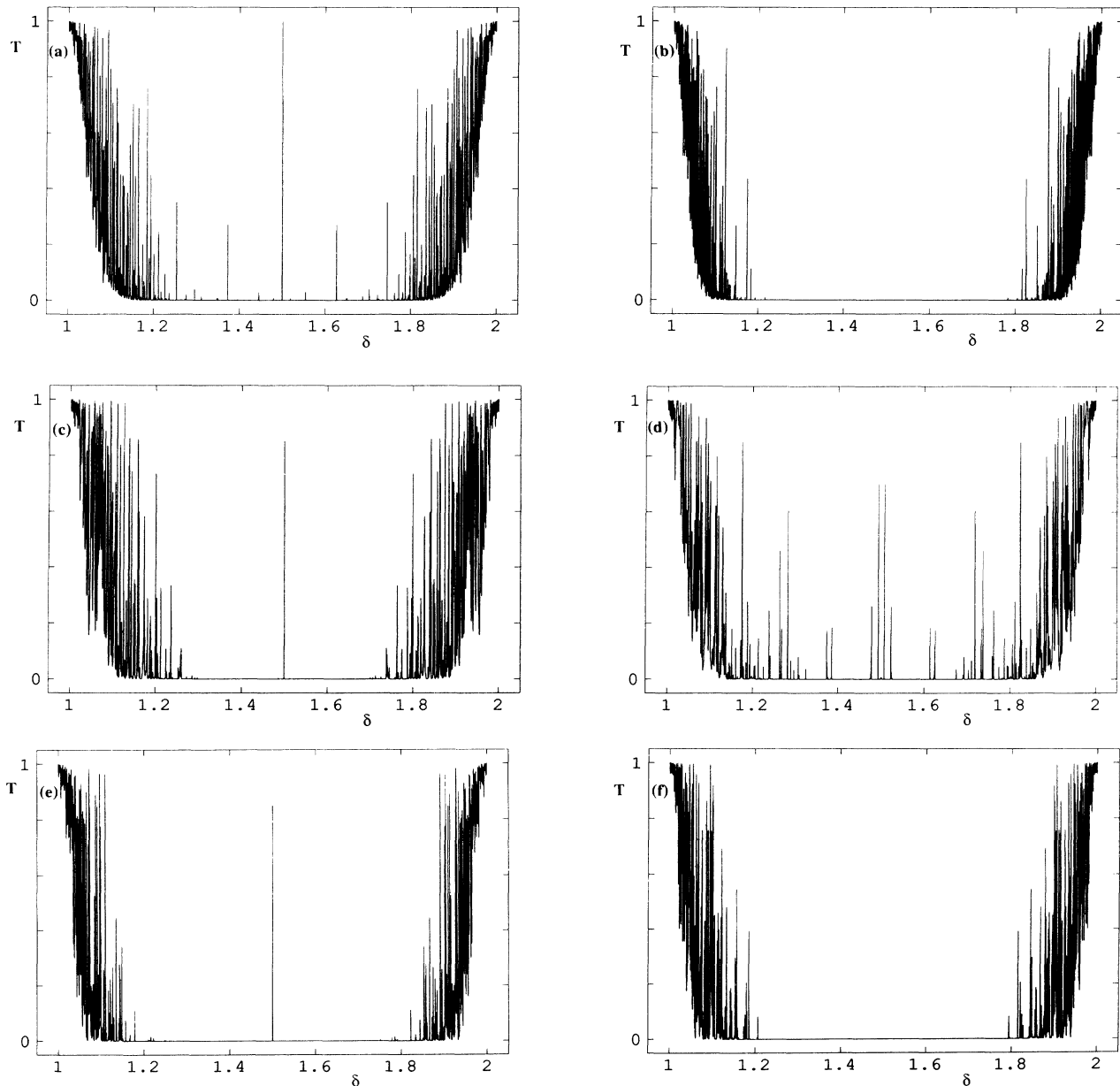

FIG. 12. The transmission coefficient T as a function of the phase δ measured in units for π for (a) a RS chain of length $N=512$, (b) a RS chain of length $N=1024$, (c) and (d) two different disordered configurations for 512 layers, and (e) and (f) same as in (c) and (d) but for 1024 layers. In all cases the ratio of the refractive indices is 1.5.

sequence was investigated. Two physical realizations of this distribution were studied: (a) an electronic tight-binding model with diagonal aperiodicity, and (b) an aperiodic dielectric multilayer composed of two kinds of layers having different refractive indices. Both systems were treated in the frame of the transfer-matrix formalism making use of nonlinear recurrence relations satisfied by the transfer matrices and their traces corresponding to successive generations of the chain. Numerical computations of the first and second moments and of the inverse participation ratio lead to the conjecture that the electronic wave functions are, in general, localized, displaying at the same time a rich self-similar structure. Also, a class of eigenfunctions was found for which a combined analytical and numerical analysis showed a qualitative change in behavior when the strength V of the amplitude of the on-site energy is varied: while, for $V=1$, these states are weakly localized, there is a countable dense set of critical subunitary values of V for which they become extended. The overall tendency towards localization of the wave functions shows that, in contrast to some other deterministic aperiodic models previously studied which present mainly critical[6] or extended[7,22] states, the Rudin-Shapiro tight-binding model behaves more closely to the disordered systems.

The influence which the localization property has on the time evolution of the electronic wave packet was numerically investigated. It was found that the existence of extended states in the critical cases can give only a subdiffusive behavior for the mean-square displacement of the wave packet and a slow decrease of the probability of return to the starting site.

The study of the optical transmission through the Rudin-Shapiro dielectric multilayer has lead to the conclusion that the electromagnetic waves are localized too. It was shown that gaps in the transmission spectra develop around some phase values when the number of layers is increased. The comparison of these results with the behavior of the binary disordered layers having the same optical parameters emphasized their strong similarities. The above-mentioned results lead to the general conclusion that the complexity of the Rudin-Shapiro distribution has in some aspects effects on the physical properties close to those of a random distribution.

ACKNOWLEDGMENTS

APPENDIX

In order to prove the recurrences appearing in Sec. I, it is useful to derive first from Eq. (2.6) the following identities:

$$\underline{B}_n\underline{A}_n^{-1}=\underline{C}_{n-1}\underline{B}_{n-1}^{-1} ,$$
$$\underline{A}_n^{-1}\underline{C}_n=\underline{A}_{n-1}^{-1}\underline{D}_{n-1} ,$$
$$\underline{D}_n^{-1}\underline{B}_n=\underline{D}_{n-1}^{-1}\underline{A}_{n-1} ,$$
$$\underline{C}_n\underline{D}_n^{-1}=\underline{B}_{n-1}\underline{C}_{n-1}^{-1} ,$$

$$(A1)$$

and

$$\underline{A}_n=\underline{B}_n^{-1}\underline{A}_{n+1}=\underline{C}_n^{-1}\underline{B}_{n+1}, \quad \underline{B}_n=\underline{A}_{n+1}\underline{A}_n^{-1}=\underline{C}_{n+1}\underline{D}_n^{-1},$$

$$(A2)$$

$$\underline{C}_n=\underline{B}_{n+1}\underline{A}_n^{-1}=\underline{D}_{n+1}\underline{D}_n^{-1}, \quad \underline{D}_n=\underline{B}_n^{-1}\underline{C}_{n+1}=\underline{C}_n^{-1}\underline{D}_{n+1}.$$

Then, by combining the first and the fourth identity of (A1), we get

$$\underline{C}_{n-2}\underline{D}_{n-2}^{-1}=\underline{A}_{n-2}\underline{B}_{n-2}^{-1} . \qquad (A3)$$

The matrix $\underline{D}_n$ can be eliminated from the above equality with the help of the last identity from (A2) and we obtain

$$\underline{C}_{n-1}=\underline{B}_{n-2}^2\underline{A}_{n-2}^{-1}\underline{C}_{n-2} . \qquad (A4)$$

The recurrence formula (2.8) is proved if we first eliminate all $\underline{C}_n$'s from (A4) by making use of the third identity appearing in (A2) and then eliminating from the resulting equation all $\underline{B}_n$'s with the help of the second equality from (A2). Equation (2.9) is the straightforward consequence of (A4) and the first relation from (A1).

In the derivation of the recurrence relation satisfied by traces (2.10), we make use of the following identity which holds for the traces of any pair $\underline{X}$ and $\underline{Y}$ of unimodular matrices or order 2:

$$\text{tr}(\underline{X}\underline{Y}+\underline{X}\underline{Y}^{-1})=\text{tr}\underline{X}\,\text{tr}\underline{Y} . \qquad (A5)$$

Then, if one takes the trace in the first two equations from (2.6) and apply Eq. (A5), we can write, using the notation introduced in Sec. II,

$$\text{tr}(\underline{B}_n\underline{A}_n^{-1})=a_n b_n-a_{n+1} ,$$
$$\text{tr}(\underline{A}_n^{-1}\underline{C}_n)=a_n c_n-b_{n+1} .$$

$$(A6)$$

By reasons of symmetry, the same equation holds if we replace the $\underline{A}_n$'s by $\underline{D}_n$'s, the $\underline{B}_n$'s by $\underline{C}_n$'s, and the $\underline{C}_n$'s by $\underline{B}_n$'s. So we can write

$$\text{tr}(\underline{D}_n^{-1}\underline{B}_n)=b_n d_n-c_{n+1} ,$$
$$\text{tr}(\underline{C}_n\underline{D}_n^{-1})=c_n d_n-d_{n+1} .$$

$$(A7)$$

Equation (2.10) is the immediate consequence of (A1), (A6), and (A7).

In order to prove formula (3.4), we assume first that the total transfer matrices corresponding to the even generations have the expression

$$\underline{A}_{2j}=\begin{bmatrix} f_j^2-1-EF_j & F_j \\ X_j & 1+G_j+EF_j \end{bmatrix}, \quad j\geq 2 , \qquad (A8)$$

where the polynomials G_j are given by the recurrence relation

$$G_{j+1} = 2^{3/2} f_{j+1} G_j - (f_{j+1} - 2^{1/2})^2, \quad j \geq 2 ,$$
$$G_2 = -8V^2(3V^2 - 1) , \tag{A9}$$

and X_j can be derived from the unimodularity condition $\det(\underline{A}_{2j}) = 1$. Then it can be shown by making use of the recurrence relation (2.8) and applying mathematical induction that Eqs. (3.4) and (A8) really hold for any j.

The existence of the periodic subsequence of sites $m_{p,q}$ discussed in Sec. III can be proven if we observe first that, according to the substitution relation (2.1), the RS sequence is built of four different words only containing 16 letters each arranged in a nonperiodic way. The transfer matrices associated to these words read

$$\underline{M}_A \underline{M}_B \underline{M}_A^3 \underline{M}_B^4 \underline{M}_A \underline{M}_B^2 \underline{M}_A \underline{M}_B^3 ,$$
$$\tag{A10}$$
$$\underline{M}_A \underline{M}_B \underline{M}_A^3 \underline{M}_B^3 \underline{M}_A \underline{M}_B \underline{M}_A^2 \underline{M}_B \underline{M}_A^3 ,$$

plus two more products obtained from the previous ones by replacing each A with B and vice versa. In the case at hand, a simple computation gives

$$\underline{M}_A \underline{M}_B \underline{M}_A^2 = \underline{M}_A \underline{M}_B^3 \underline{M}_A \underline{M}_B \underline{M}_A^2 \underline{M}_B \underline{M}_A^3$$

$$= -\underline{M}_A \underline{M}_B^4 \underline{M}_A \underline{M}_B^2 \underline{M}_A \underline{M}_B^3 = \begin{bmatrix} -1 & 0 \\ -\sqrt{2} & -1 \end{bmatrix} ,$$

$$\tag{A11}$$

and the symmetric relation obtained from (A11) with the exchange $A \leftrightarrow B$ and changing the sign of $-\sqrt{2}$. Equation (A11) shows that, when successively applying the above matrices to the initial vector U_1, the amplitude ψ_1 is reproduced (up to the sign) on the sites $m_{p,q}$.

[1] D. S. Shechtman, I. Blech, D. Gratias, and J. W. Cahn, Phys. Rev. Lett. **53**, 1951 (1984).

[2] P. J. Steinhardt and S. Ostlund, *The Physics of Quasicrystals* (World-Scientific, Singapore, 1987).

[3] S. Aubry, and G. André, Ann. Isr. Phys. Soc. **3**, 133 (1980).

[4] D. R. Grempel, S. Fishman, and R. E. Prange, Phys. Rev. Lett. **49**, 833 (1982). ·

[5] J. P. Allouche, and M. Mendes-France, J. Phys. (Paris) Colloq. **47**, C3-63 (1986).

[6] M. Kohmoto, L. P. Kadanoff, and C. Tang, Phys. Rev. Lett. **50**, 1870 (1983); S. Ostlund, R. Pandit, D. Rand, H. J. Schellnhuber, and E. G. Siggia, *ibid.* **50**, 1873 (1983); A. Sütö, Commun. Math. Phys. **111**, 409 (1987).

[7] M. Severin, M. Dulea, and R. Riklund, J. Phys.: Condens. Matter **1**, 8851 (1989).

[8] M. Kohmoto, B. Sutherland, and K. Iguchi, Phys. Rev. Lett. **58**, 2436 (1986).

[9] R. Riklund and M. Severin, J. Phys. C **21**, 3217 (1988).

[10] M. Dulea, M. Severin, and R. Riklund, Phys. Rev. B **42**, 3680 (1990).

[11] W. Rudin, Proc. Am. Math. Soc. **10**, 855 (1959); H. S. Shapiro, Master's thesis, Massachusetts Institute of Technology, 1951.

[12] M. Queffélec, *Substitution Dynamical Systems-Spectral Analysis*, Lecture Notes in Mathematics, Vol. 1294 (Springer, Berlin, 1987).

[13] A. Aldea and M. Dulea, Phys. Rev. Lett. **60**, 1672 (1988).

[14] J. M. Luck, Phys. Rev. B **39**, 5834 (1989).

[15] C. Godrèche and J. M. Luck, J. Phys. A **23**, 3769 (1990).

[16] M. Kolár and F. Nori, Phys. Rev. B **42**, 1062 (1990).

[17] *Handbook of Mathematical Functions*, edited by A. Abramovitz and I. A. Stegun (Dover, New York, 1965).

[18] S. Abe and H. Hiramoto, Phys. Rev. A **36**, 5349 (1987); H. Hiramoto and S. Abe, J. Phys. Soc. Jpn. **57**, 230 (1988); **57**, 1365 (1988).

[19] D. H. Dunlap, H-L. Wu, and P. W. Phillips, Phys. Rev. Lett. **65**, 88 (1990).

[20] I. Guarneri, Europhys. Lett. **10**, 95 (1989).

[21] P. W. Anderson, Phys. Rev. **109**, 1492 (1958).

[22] F. Axel and J. Peyrière, C. R. Acad. Sci. Paris **306**, 179 (1988); J. Bellissard, in *Number Theory and Physics*, edited by J. M. Luck, P. Moussa, and M. Waldschmidt, Springer Proceedings in Physics, Vol. 47 (Springer-Verlag, Berlin, 1990), p. 140; R. Riklund, M. Severin, and Y. Liu, Int. J. Mod. Phys. B **1**, 121 (1987).